

Supplementary Figures and Tables

AcrB: a mean, keen, drug efflux machine

Jessica Kobyłka*, Miriam S. Kuth*, Reinke T. Müller*, Eric R. Geertsma, Klaas M. Pos⁺

Institute of Biochemistry, Goethe-University Frankfurt, Max-von-Laue-Str. 9, D-60438 Frankfurt am Main, Germany.

*These authors contributed equally

+Corresponding author. Tel: +49-(0)69-798 29251; Fax: +49-(0)69-798 29201; E-mail: pos@em.uni-frankfurt.de

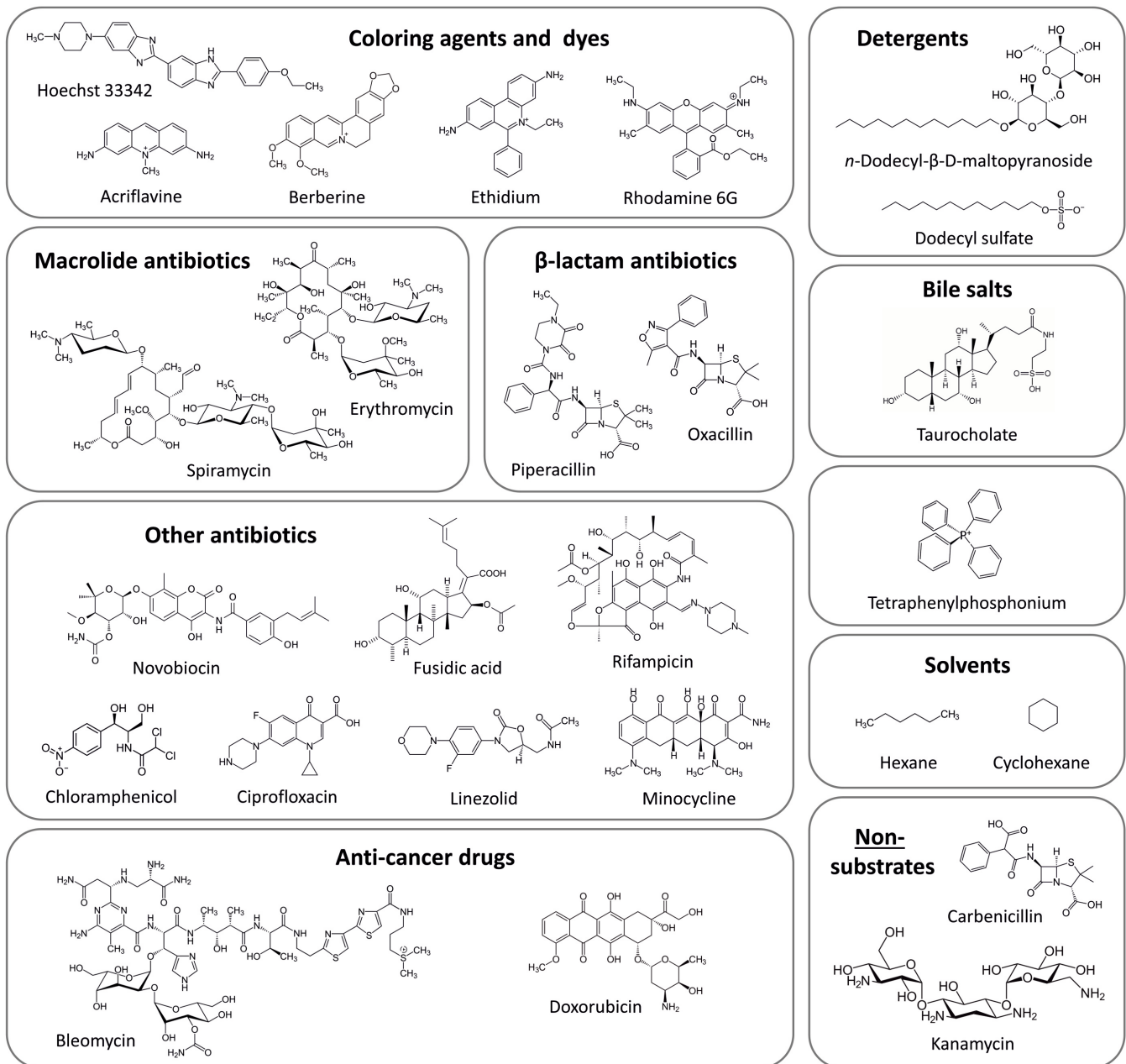


Figure S1: Substrates of the AcrAB-TolC multidrug efflux pump. The substrates of the AcrAB-TolC multidrug efflux pump display large diversity in structure and size. The spectrum includes coloring agents (dyes), macrolides, β-lactams and other classes of antibiotics including aminocoumarines (novobiocin), rifamycins (rifampicin), quinolones (ciprofloxacin), oxazolidones (linezolid) and tetracyclines (minocycline). In addition, AcrAB-TolC transports anti-cancer drugs, detergents, bile salts and solvents. A common physicochemical feature between these substrates is the presence of hydrophobic moieties. More hydrophilic compounds such as bi-anionic β-lactams (e.g. carbenicillin) and aminoglycosides (e.g. kanamycin) are not or poorly transported by the AcrAB-TolC pump but have been shown to be substrates of the closely related AcrAD-TolC multidrug efflux pump.

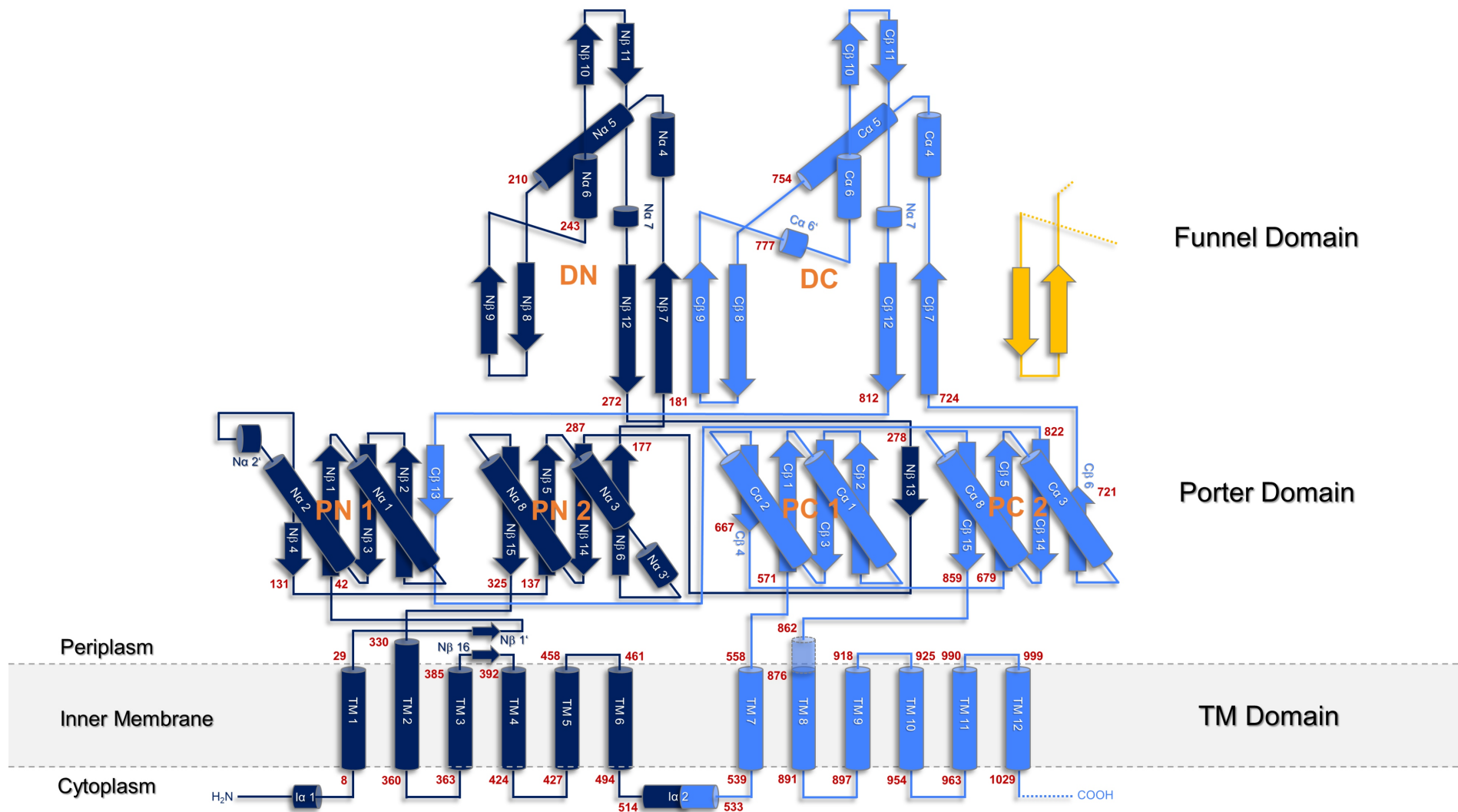


Figure S2: Secondary structure of the AcrB monomer: The AcrB monomer can be structurally subdivided into three domains: a funnel domain (aka docking domain), a porter domain and a transmembrane (TM) domain. The funnel domain can be further subdivided into two subdomains, DN and DC. The porter domain is subdivided into the four subdomains PN1, PN2, PC1 and PC2. Helix $\alpha 2$ is the cytoplasmic cross- α -helix, which separates the N-terminal part (indicated in dark blue) and the C-terminal part (indicated in light blue) of the protein. The marked sheets (β) and helices (α) within the funnel and porter domain belong to the N-terminal (dark blue) and C-terminal (light blue) part. The amino acid positions are given in dark red numbers next to the corresponding elements for better orientation. Furthermore, the intermonomer connecting loop from the next monomer is colored in yellow.

a)

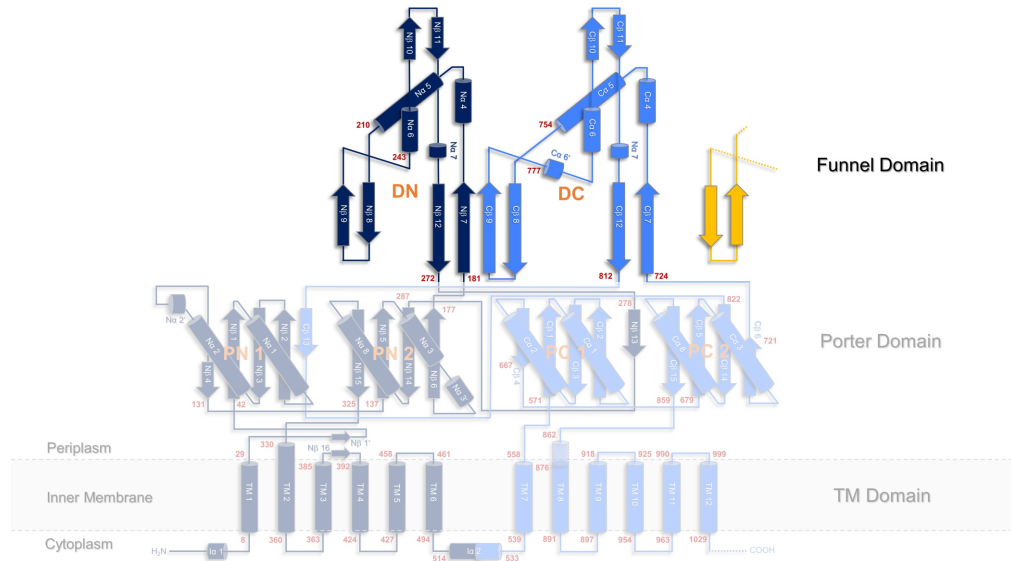
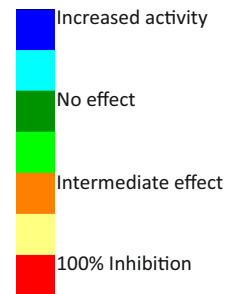
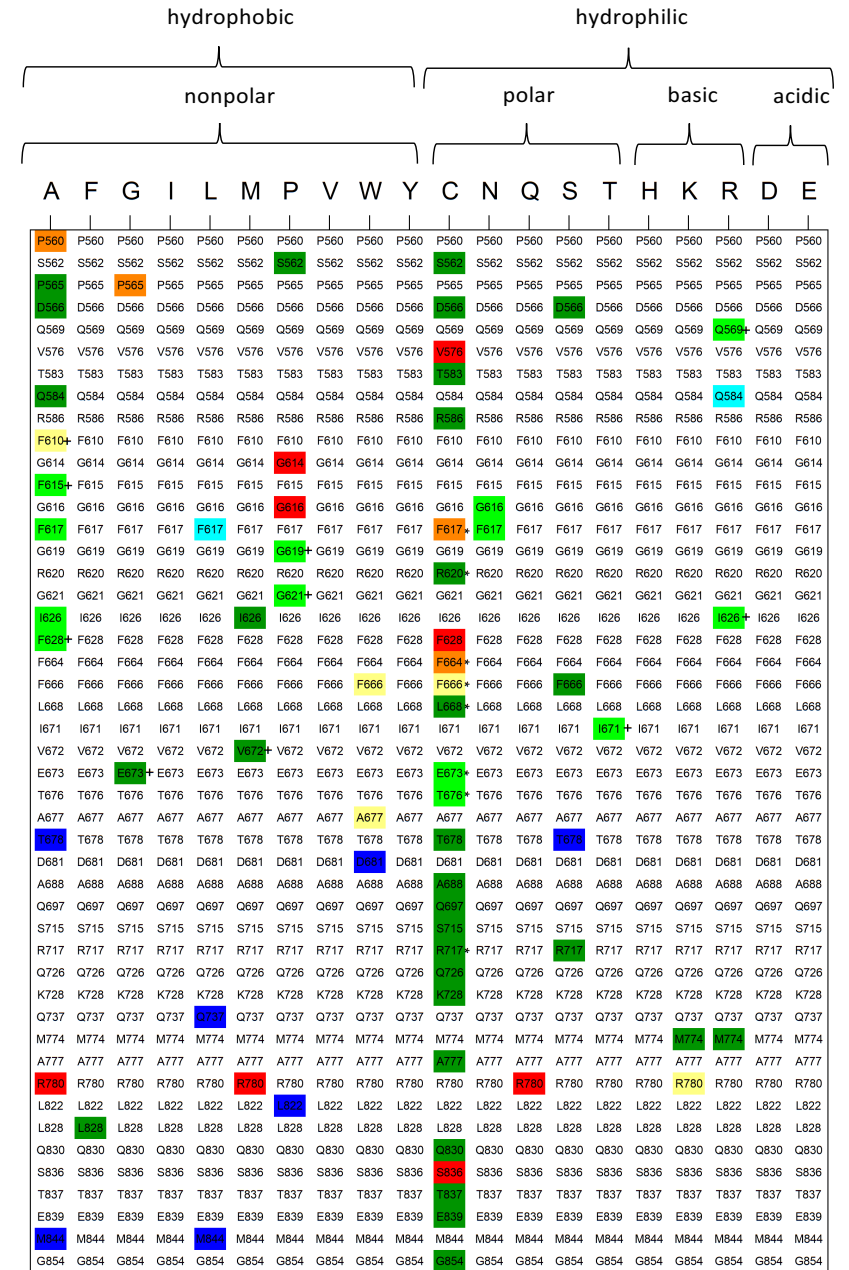


Figure S4: Single substitutions in the Funnel Domain: **a)** Presents the secondary structure of the AcrB monomer with highlighted funnel domain. **b)** Heat map providing all positions (from N- to C-terminus) in the funnel domain on the Y-axis. The substituted amino acids are presented on the X-axis, sorted by hydrophobic and hydrophilic (subdivided into polar, basic and acidic) amino acid residues. Non-colored positions were not substituted. Substituted positions are color-coded based on their activity compared to the wildtype, see legend next to the heat map. Detailed activities, regarding the different substrates are described in Table S2. (Positions marked with * : Cys-substitutions in wildtype AcrB background (**not** cysteine-less); positions marked with +: additional effects with regard to activities, see table S3)

b)



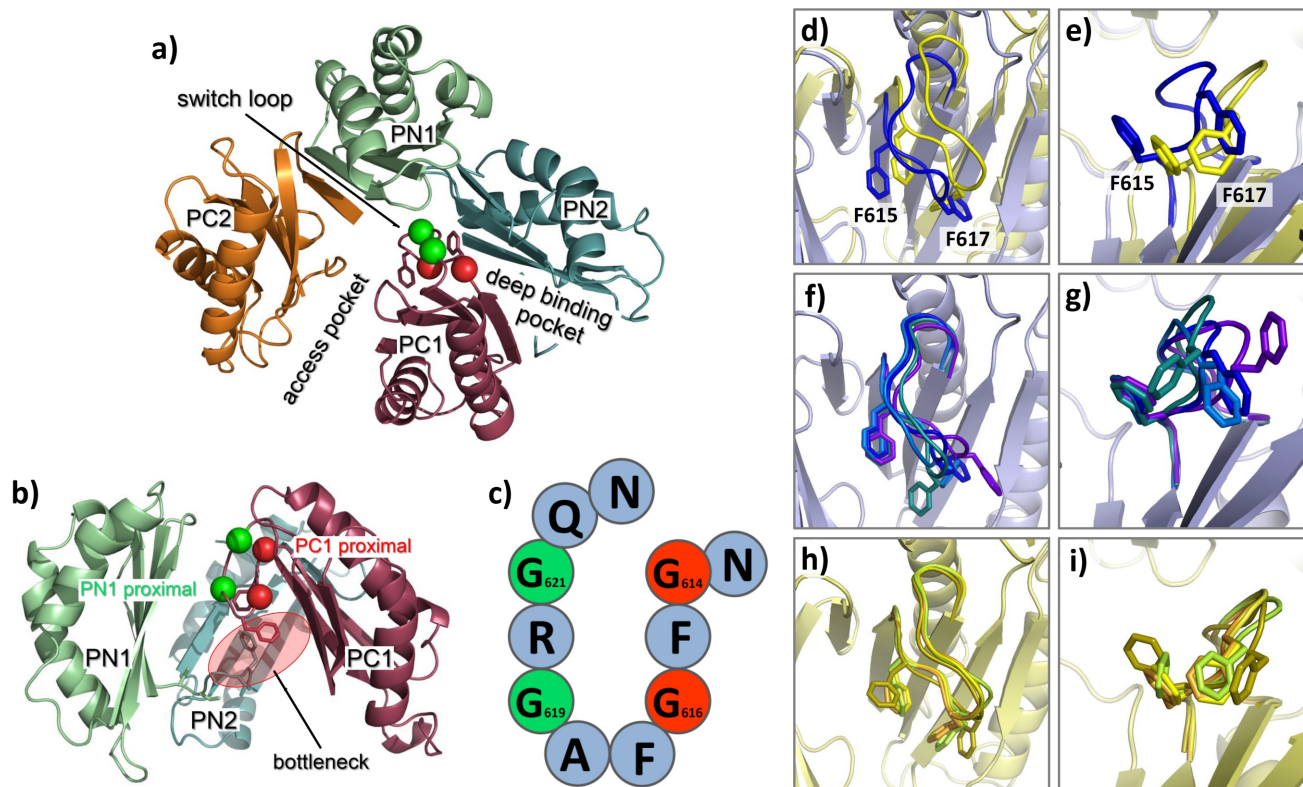


Figure S5: The switch loop as a flexible structural element between AP and DBP: The switch loop is part of the PC1 subdomain, localized between the AP and the DBP (a) and part of a bottleneck between both pockets (b). This structural motive comprises eleven amino acid residues with four symmetrically arranged glycine residues, which due to their localization were classified as PC1 (G614, G616) (red) and PN1 proximal (G619, G621) (green), respectively (a, b, c). Depending on the conformational state and the substrates present, the switch loop can adopt different conformations (d-i). The switch loops (including the F615 and F617 side chains) and the β -sheets of the PC1 domains of different, superimposed L and T protomers are shown from a side (d, f, h) and a bottom (viewed from the membrane) perspective (e, g, i). The DBP is located on the right and the AP on the left of the switch loops. As can be seen by comparison of the L (blue) and T (yellow) states in the AcrB/minocycline costructure, the switch loop is shifted towards the AP during the L-T transition, contributing to a larger DBP. The comparison of different L switch loops including the apo protomer (blue, pdb: 4DX5) and the rifampicin (teal, pdb: 3AOB), erythromycin (purple, pdb: 3AOC) and doxorubicin co-structures (marine, pdb: 4DX7) indicates high conformational flexibility at the tip of the loop close to F617 (f, g). The switch loops from the T states, in contrast, appear to be far more invariant, as comparison of the minocycline (yellow, pdb: 4DX5), doxorubicin (orange, pdb: 4DX7), puromycin (lemon, pdb: 5NC5) and rhodamine 6G (olive, pdb: 5ENS) AcrB co-structures suggest (h, i).

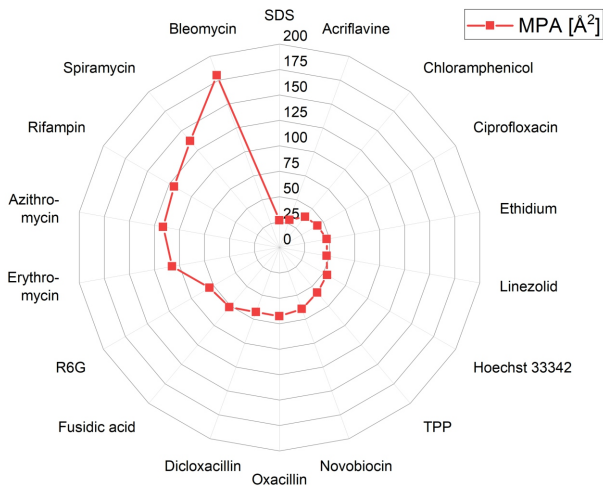
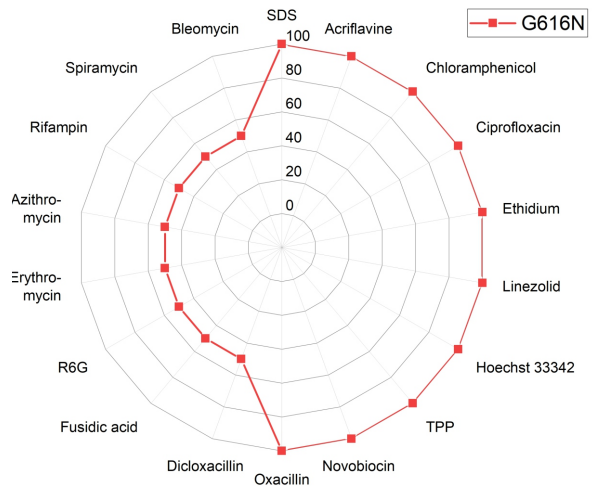
A**B**

Figure S6 : Correlation of the substrate minimal projection area (MPA) and efflux activity of the G616N variant: MPAs of tested substrates given in (A); sorted by MPA [Å²] clockwise in ascending order in both graphs (A) and (B). Efflux activities of the G616N variant with different substrates are given in % of WT activity (B). A decrease in efflux activity of the G616N variant can be correlated with an increase of the MPA as substrates with an MPA >75 Å² are transported with 50% lower effectivity¹.

	R6G	SDS	TPP	Ery	Oxa	Eth	Lin	Nov
D407N	1	1	1	1	1	1	1	1
Aswloop	2	1	1	1	1	2	1	1
WT	32	512	64	8	128	32	8	16
F615A	16	512	128	4	32	16	8	4
F617A	32	512	128	8	64	32	8	4
F615A F617A	16	16	128	8	32	16	8	2
G614P	2	1	1	1	1	2	1	0,5
G614P F615A	2	8	16	2	8	4	1	2
G614P F617A	1	2	2	0,5	1	0,5	1	1
G614P F615A F617A	2	16	32	4	16	8	1	1
G616P	2	1	2	1	2	1	1	1
G616P F615A	2	2	2	1	4	1	1	1
G616P F617A	4	2	8	2	8	2	2	2
G616P F615A F617A	16	256	32	8	64	8	4	4
G619P	32	256	32	4	16	8	2	2
G619P F615A F617A	16	512	64	8	64	8	4	4
G616P G619P	2	1	1	1	1	2	1	1
G616P G619P F615A F617A	8	32	16	2	32	4	2	2

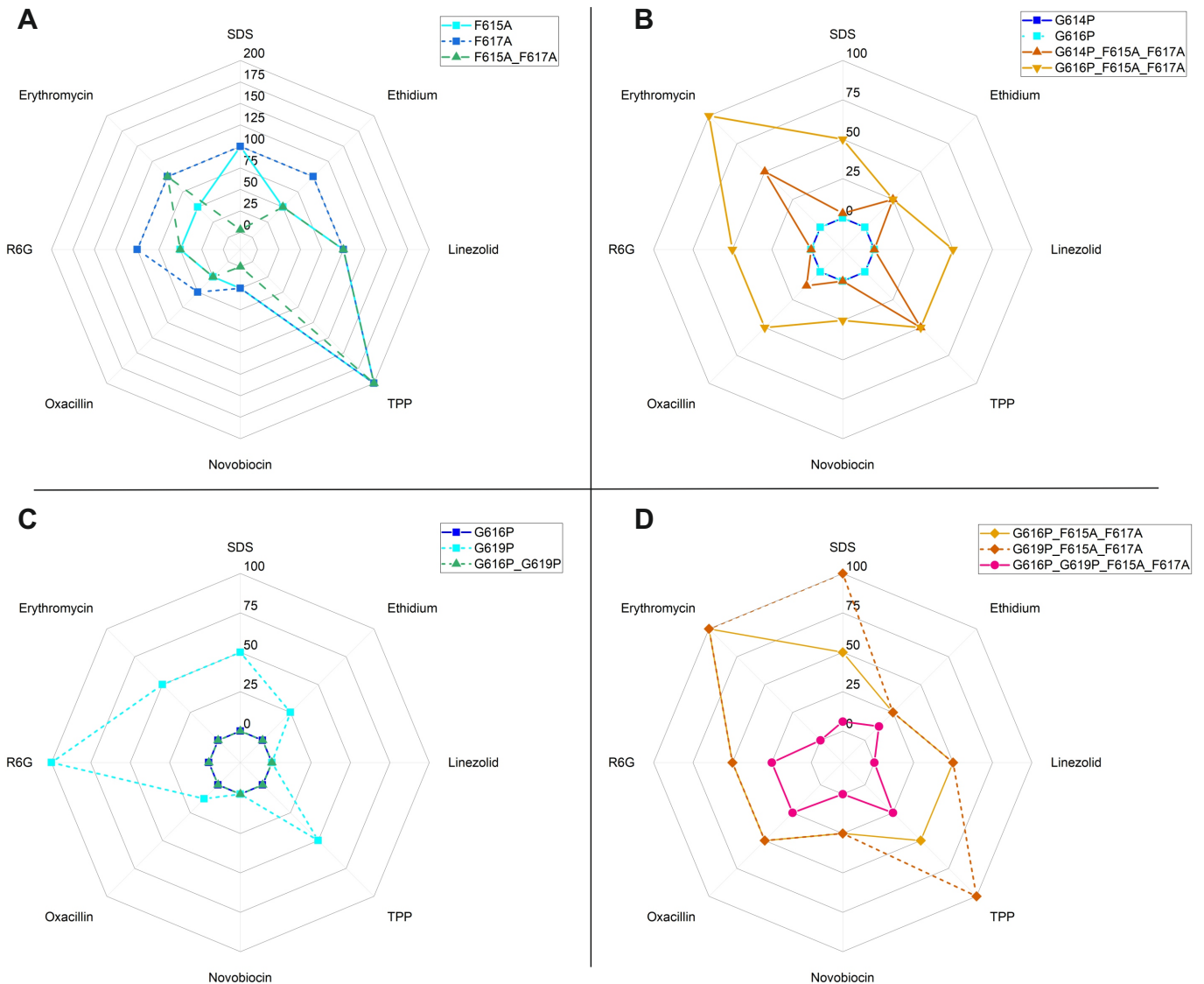


Figure S7 : Switch loop substitution causing AcrB inactivation and suppressor substitutions: MIC values for the Gly-to-Pro and Phe-to-Ala single and multiple substitution switch loop variants were determined for SDS, ethidium, linezolid, TPP, novobiocin, oxacillin, R6G and erythromycin (Table shown, adapted from Müller et al., 2017²). Substitutions causing one dilution step differences in MIC compared to wildtype activities are considered as having no effect on activity. **(A)** Single or double substitution of F615 and F617 with alanin affected resistance towards tested drugs only slightly, except for SDS and novobiocin. **(B)** Whereas single G614P or G616P substitution variants were completely inactive, activity could be regained by additional F615A and/or F617A substitution. **(C)** The G619P variant shows a substrate-dependent mixed resistance phenotype, while the double substitution variant G616P_G619P is completely inactive. **(D)** The inactive phenotypes of G616P and/or G619P substitution variants are rescued by additional F615A and F617A substitutions (G616P_F615A_F617A, G619P_F615A_F617A and G616P_G619P_F615A_F617A). Activities of single substitution variants are indicated in blue symbols, for double, triple and quadruple substitution variants in green, orange and magenta, respectively. Substrates are sorted by MPA [Å²] clockwise in ascending order.

Table S3: Comments on the marked positions (with a plus (+)) in the heat maps of the funnel, porter and TM domain (Figure 7 and Figure S3-S4).

Funnel Domain		Porter Domain		TM Domain	
Mut.	Comment	Mut.	Comment	Mut.	Comment
F453C	inhibition for Nalidixic acid; no effect for all other substrates (erythromycin, novobiocin, minocycline)	Q569R	inhibition with cefamandole	I38F	increased activity for clarithromycin; 100% inhibition for chloramphenicol; Intermediate effect for linezolid, cefuroxime, oxacillin, levofloxacin, pyronin Y; No effect for others
L886G	with ethidium (efflux transport = inhibition)	F610A	no effect with: ethidium, propidium chloride, doxorubicin; increased effect with NPN	D101C	inhibition for chloramphenicol, tetracycline, nalidixic acid, crystal violet; Intermediate effect for erythromycin, acriflavine, R6G, benzalkonium; no effect for others
W895G	with ethidium (efflux transport = inhibition)	F615A	excluded data from PMID 26240069 (inhibition for: erythromycin, novobiocin, minocycline and nalidixic acid)	V105C	no effect for novobiocin, Intermediate effect for erythromycin, ethidium, R6G, TPP; inhibition for others
		G619P	inhibition with linezolid and novobiocin	N109C	inhibition for chloramphenicol, tetracycline, nalidixic acid, norfloxacin, crystal violet; Intermediate effect for erythromycin, acriflavine, R6G, benzalkonium; no effect for others
		G621P	inhibition with linezolid and novobiocin	P116C	inhibition for chloramphenicol, tetracycline, nalidixic acid, crystal violet; intermediate effect for acriflavine, benzalkonium; no effect for others
		I626R	increased activity with aztreonam, carbenicillin and sulbenicillin	F178A	efflux assay with ethidium: no effect

		F628A	with erythromycin and ethidium	L219A	also: no effect visible
		I671T	inhibition with erythromycin and ethidium	P223A/V/Y/N	also: no effect visible
		V672M	increased activity with clarithromycin	P224T	also: increased activity (clarithromycin)
		E673G	efflux transport with Nile Red + pyrene maleimide = intermediate	L230A	no effect for R6G
				Y327A	increased activity for Rhodamine 6G; inhibition for tetracycline, acriflavine, benzalkonium
				T329A	no effect visible

References

1. Cha H.J., R.T. Müller & K.M. Pos. 2014. Switch-loop flexibility affects transport of large drugs by the promiscuous AcrB multidrug efflux transporter. *Antimicrobial Agents and Chemotherapy* **58**: 4767–4772.
2. Müller R.T., T. Travers, H. Cha, *et al.* 2017. Switch Loop Flexibility Affects Substrate Transport of the AcrB Efflux Pump. *Journal of Molecular Biology* **429**: 3863–3874.